PROCEEDINGS OF SCIENCE

# Effect of gravitational lensing on supernova cosmology

**Hinako Sakakibara,** [a] **Atsushi J. Nishizawa**[*b,a]**, Masamune Oguri,**[c,d,e] **Masayuki Tanaka,**[f] **Bau-Ching Hsieh**[g] **and Kenneth C. Wong**[e]

[a] *Department of Physics, Nagoya University, Furocho, Chikusa, Nagoya 464-8602, Aichi, Japan*
[b] *Institute for Advanced Research, Nagoya University, Furocho, Chikusa, Nagoya 464-8602, Aichi, Japan*
[c] *Research Center for the Early Universe, University of Tokyo, Tokyo 113-0033, Japan*
[d] *Department of Physics, University of Tokyo, Tokyo 113-0033, Japan*
[e] *Kavli Institute for the Physics and Mathematics of the Universe (Kavli IPMU, WPI), University of Tokyo, Chiba 277-8582, Japan*
[f] *National Astronomical Observatory Japan, 2-21-1 Osawa, Mitaka, Tokyo 181-8588, Japan*
[g] *Academia Sinica Institute of Astronomy and Astrophysics, P.O. Box 23-141, Taipei 10617, Taiwan*
*E-mail:* atsushi.nishizawa@iar.nagoya-u.ac.jp

***Aim:*** As a measurement of distance modulus for type Ia supernovae becomes more stringent, it is important to study various systematics for the unbiased measurement of cosmological parameters. In this paper, the effects of gravitational lensing magnification on the measurement of supernovae distance modulus and estimation of cosmological parameters are presented.

***Method:*** We use Hyper Suprime-Cam survey data to estimate the interbening large-scale structure. Two distinct methods are applied; one based on weak lensing mass reconstruction and the other based on the galaxy distribution. Then those estimations are converted to predict the possible magnification of individual supernova.

***Results:*** We find a very weak correlation between the Hubble residuals and magnification and that the $\Omega_m$ and dark energy parameter $w$ alters best fit values by $\mathcal{O}(1)\%$ level.

***Conclusion:*** The effect of magnification can be vanishingly small given the current SNLS supernovae sample; however, it becomes important in the era of LSST and WFIRST where the number of supernovae is dramatically increase.

*The 4th KMI International Symposium (KMI2019)*
*18-20, February 2019*
*Nagoya, Japan*

[*] Speaker.

## 1. Introduction

Type Ia supernav (SN) is a useful tool to probe cosmological model through the luminosity distance. Since the absolute magnitude of IaSN is well calibrated using the light curve profile and color information, given the redshift of the SNe, we can predict the luminosity distance to the SNe. Particularly it is sensitive to the amount of dark energy at $z < 1$ and equation of state parameter of dark energy $w$. After the first constraints on the accelerating rate of the Universe, Garnavich et al. (1998); Riess et al. (1998); Perlmutter et al. (1999), number of constraints on dark energy parameters are placed Filippenko et al. (2001); Astier et al. (2006); Frieman et al. (2008); Dawson et al. (2009); Grogin et al. (2011).

If we compare the measured distance modulus with the ΛCDM prediction, the data is scattered around prediction. One possible explanation is that there still be a diversity of Ia SNe which cannot absorbed in the color and magnitude correction for the light curve profile. Another possible source of this scatter may arise from the gravitational lensing magnification due to the intervening large-scale structure (e.g. Frieman, 1996). The SNe fluxes are magnified where the mass distribution along the line of sight is clustered, while they are demagnified where lower density region.

In this work, we investigate magnification of SNe Ia fluxes using HSC galaxy photometric catalog. We estimate magnification by two different methods: one measures convergence by mass reconstruction using galaxy shape catalog, while the other measures magnification from galaxy distribution assuming that galaxy resides dark matter halo with an NFW profile. We also investigate the impact of magnification effect on the cosmological parameter estimation by comparing the results with and without the magnification correction to the distance modulus.

## 2. Data sets

**Supernova Legacy Survey 3-year sample**

We use Supernova Legacy Survey (SNLS) 3-year data products for SNe Ia analysis (Guy et al., 2010). The SNLS sample has both redshift and light curve data with multi photometric bands. The observed field of SNLS is distributed at CFHTLS deep fields of `D1` to `D4` roughly span 1 square degree field on the sky. The photometric data of SNe are taken by CHTL and the spectra are taken by VLT, Gemini and Keck telescopes.

The SNLS 3-year data sets are used to constrain cosmological parameters $\Omega_{\rm m0} = 0.211 \pm 0.034(\mathrm{stat.}) \pm 0.069(\mathrm{sys.})$ Guy et al. (2010) and $w = -0.91^{+0.16}_{-0.20}(\mathrm{stat.})^{+0.07}_{-0.14}(\mathrm{sys.})$ Conley et al. (2011). There are two empirical methods to model the SN light curve, SLAT2 (Guy et al., 2007) and SiFTO (Conley et al., 2008) and they are summarized in Guy et al. (2010). We follow Guy et al. (2010) to make a clean sample of SNe which is least affected by individual feature of the SNe, such as dust extinction. Our final sample include 231 SNe.

**Hyper Suprime-Cam**

HSC is the wide field optical imaging camera installed on the prime focus of the Subaru Telescope (Miyazaki et al., 2018). The HSC collects the precise shape and photometry of galaxies. In this work, we use photometric redshift for S17A release from deep and ultra-deep fields and S16A galaxy shape catalog from wide layers of full-depth-full-color (FDFC) regions overlapped with deep and ultra-deep fields (Mandelbaum et al., 2018).



PoS(KMI2019)043

We use two different photometric redshift catalogs: one from template fitting, `Mizuki` (Tanaka, 2015) and the other based on the empirical method, `DEmP` (Hsieh & Yee, 2014). The photometric redshift accuracy and methodology are summarized in Tanaka et al. (2018).

The HSC and SNLS fields are partially overlapped at `D1, D2` and `D3` fields, which contains 158 sample selected SNe. We further remove 5 SNe located near the very bright stars, with the separation closer than 0.8 arcmins Eventually, the number of SNe we use in our analysis is 153.

## 3. Estimation of magnification

**Convergence measure**

Here we revisit the mass reconstruction using the weak lensing shear estimation (e.g. Oguri et al., 2018). The magnification can be defined using the Jacobian matrix

$$\mu_{\rm lens} = \frac{1}{\det\mathscr{A}} = \frac{1}{(1-\kappa)^2 - |\gamma|^2} \approx 1 + 2\kappa \equiv 1 + \delta\mu_{\rm lens}, \tag{3.1}$$

where $\kappa$ and $\gamma$ is lensing convergence and shear. The last approximation is only valid in the weak lensing limit where we are working on.

We use HSC shear catalog (Mandelbaum et al., 2018) with the smoothing scale to reconstruct the convergence field. Since the HSC shear catalog only overlaps with `D1` field, the total number of SNe used for this convergence measurement is limited to 52. For the source galaxy redshift, we use photometric redshift catalog of `Mizuki`. For each SN, we reconstruct the surface density using galaxies in the `D1` whose redshift satisfies

$$z_{p,\rm best} < z_{SN}. \tag{3.2}$$

The average number of galaxies available is $\bar{n}_{\rm gal} = 0.6\,\mathrm{arcmin}^{-2}$ for $z_s = 0.2$ and $\bar{n}_{\rm gal} = 13\,\mathrm{arcmin}^{-2}$ for $z_s = 1.0$.

**Direct measure**

We also measure the magnification in an independent method. We consider that the SN flux is magnified at the position of foreground galaxies in a single lens approximation. We assume that the galaxy has a spherical profile, $\rho(r)$. The projected mass of the galaxy along the line of sight is then,

$$\Sigma(r_\perp) = \int \rho^{\rm NFW}\left(\sqrt{r_\parallel^2 + r_\perp^2}\right) \mathrm{d}r_\parallel. \tag{3.3}$$

The convergence and two shear components induced by the mass associated with the galaxy are given by (Kaiser & Squires, 1993),

$$\kappa(\theta) = \Sigma_{\rm cr}^{-1}\Sigma(r_\perp = D_l\theta), \qquad \gamma(\theta) = \frac{1}{\pi}\int_{\mathbb{R}^2} \mathscr{D}(\theta-\theta')\kappa(\theta')\mathrm{d}^2\theta'. \tag{3.4}$$

The shear and convergence can be analytically calculated, once assumed the mass profile of the galaxy (Takada & Jain, 2003a,b).

To complete our model, we assume that the galaxy has an NFW profile. Given the virial mass of the halo, the concentration can be given by Duffy et al. (2008), $c_{200}(z) = 5.71(M_{200c}/2\times 10^{12}h^{-1}M_\odot)^{-0.084}(1+z)^{-0.47}$, which is valid over wide range of redshifts, $0 < z < 2$ and masses $11 < \log(M/M_\odot h^{-1}) < 15$.

The halo virial mass of each galaxy is estimated from the stellar mass taken from the photometric redshifts catalog of HSC. Given the stellar mass of the galaxy, the halo mass can be derived from the stellar to halo mass relation (Behroozi et al., 2010). In order to incorpolate the photo-z uncertainty, the critical surface mass density is convolved by the photo-z probability function (Mandelbaum et al., 2008)

$$\Sigma_{\rm cr}^{-1} \rightarrow \left\langle \Sigma_{\rm cr}^{-1} \right\rangle = \int_0^{z_s} P(z_l)\Sigma_{\rm cr}^{-1}(z_l, z_s)\mathrm{d}z_l \left[\int P(z)\mathrm{d}z\right]^{-1} \tag{3.5}$$

Total amount of magnification can then be evaluated by multiplying over all the foreground galaxies,

$$\log \mu_{\rm lens}^{\rm tot} = \sum_i \log \mu_{{\rm lens},i}(\theta_i) + \mathscr{M}, \tag{3.6}$$

where $\mu_{{\rm lens},i}$ is the magnification by $i$-th galaxy, and $\mathscr{M}$ is an average magnification of the Universe. The average magnification $\mathscr{M}$ can be determined so that $\langle \log \mu_{\rm lens}^{\rm tot} \rangle = 0$ averaged over 1000 random line of sight in our observation fields.

**Foreground selection**

For the direct measure of magnification, we need to identify the galaxies lying in front of the SNe. We first identify the host galaxies using the weighted separation, $\theta_w \equiv \theta/M_i$ where $\theta$ is an angular separation between SN and candidate host galaxy and $M_i$ is an $i$ band absolute magnitude of each galaxy. We remove the host galaxy from the magnification measurement. Second, we identity the foreground galaxies, which are separated less than virial radius, $\theta < r_{\rm vir}/D_l(z_p)$ from the SN. If we assume that the dark matter halo is truncated at the virial radius, only the shear contributes to the magnification outside the $r_{\rm vir}$ and they are small enough to be negligible.

## 4. Results

Here we describe our results of the correlation between magnification and Hubble residual and the cosmological parameter estimation after correcting for the magnification.

### 4.1 correlation between Hubble residual and magnifications

We expect that if the all the scatter of Hubble residual around ΛCDM prediction $\Delta\mu \equiv \mu^{\rm obs} - \mu^{\Lambda{\rm CDM}}$ is explained by the magnification by the intervening large-scale structure, the magnification and Hubble residual can be related as

$$\Delta\mu = -2.5\log_{10}(1+\delta\mu_{\rm lens}) \approx -1.086\,\delta\mu_{\rm lens}. \tag{4.1}$$

We fit the $\Delta\mu - \delta\mu^{\rm lens}$ relation with the linear function and find that $\Delta\mu = (0.187 \pm 0.364)\delta\mu_{\rm lens} + (-0.013 \pm 0.013)$ if we obtain the magnification from the convergence measurement. We also quantify the correlation using correlation coefficient and find that $r = 0.032 \pm 0.144$ which meas the detecting the correlation between Hubble residual and magnification is negative. This is due to the noisy measurement of the convergence field. To evaluate the noise, we employ exactly same analysis with randomly rotated shear catalog and find that our measured signal is fully consistent with the random noise. Another reason of no correlation is finite size of smoothing of the convergence field which is inevitable to avoid the divergence of the estimator. Since the magnification

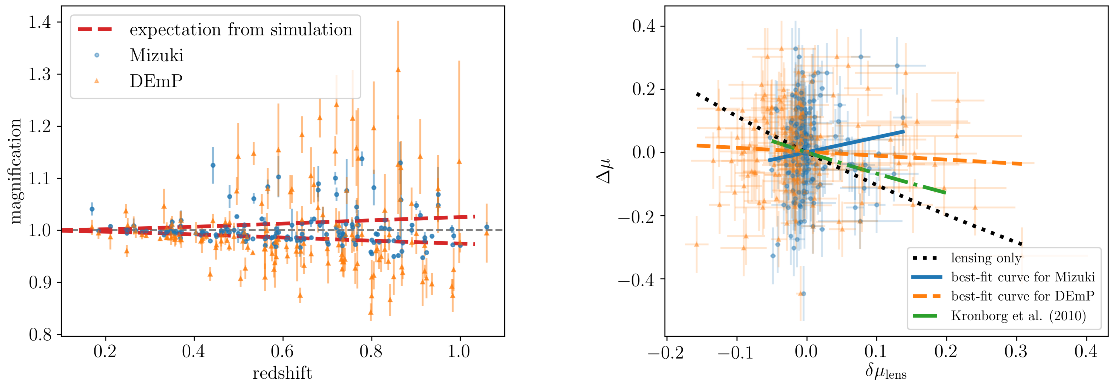


**Figure 1:** Figures quoted from Sakakibara et al. (2019). (Left) Magnification $\mu_{\rm lens}$ as a function of redshift of SNe. Blue circles and orange triangles are for `Mizuki` and `DEmP`, respectively and red dashed line shows the 68 percentile of expectation from ray-tracing simulation. (Right) Relation between Hubble residual and magnification from direct measure. Blue solid, orange dashed and black dotted lines show the fitting curve for `Mizuki` and `DEmP`, and Eq. (4.1). The green dashed-dotted line is from Kronborg et al. (2010).

relies on local structure along the line of sight, this smoothing may wash out the correlated signal. For these reasons, we do not use magnification derived from convergence in the latter analysis.

The best fitting values to the Hubble residual and magnification from direct measurement are $\Delta\mu = (0.473 \pm 0.221)\delta\mu_{\rm lens} + (0.000 \pm 0.007)$ for `Mizuki`and $\Delta\mu = (-0.125 \pm 0.095)\delta\mu_{\rm lens} + (0.002 \pm 0.007)$ for `DEmP`, respectively. Figure 1 shows the measured magnification as a function of redshift for `Mizuki`and `DEmP`compared with the ray-trace simulation (Takahashi et al., 2017). It can be seen that the `DEmP`has larger scatter of magnification because `DEmP`tends to have larger stellar mass measurement compared with `Mizuki`which gives larger flux amplification. Furthermore, larger stellar mass results in larger virial radius which may contribute to multiple line of sight SNe. We also show the correlation between Hubble residual and magnification from direct measure in the right panel of Figure 1. While the `DEmP`shows negative correlation with Hubble residual, `Mizuki`indicates slightly positive correlation. The correlation coefficients are $r = 0.070 \pm 0.081$ for `Mizuki`and $r = -0.037 \pm 0.082$ for `DEmP`, which are slightly inconsistent with the previous work (Kronborg et al., 2010). For both photo-z codes, we do not exclude the no correlation (Sakakibara et al., 2019).

### 4.2 Estimation of cosmological parameter

Given the measurement of magnification for individual SN, now we see the effect of magnification on the measurement of cosmological parameters. As we mentioned in the previous section, we focus on the magnification from direct measure. We correct the distance modulus for the magnification before fitting to the ΛCDM prediction. As in the usual regression, we estimate absolute magnitude and other correction parameters $\alpha, \beta$ with cosmological parameters of interest. Table 1 show the best fitting values of cosmological and other nuisance parameters before and after correcting for the magnification. Figure 2 presents two dimensional constraints on $\Omega_m$ and $w$ parameters marginalized over other nuisance parameters. For the `Mizuki`, the cosmological parameters are

| | Mizuki | | DEmP | |
|---|---|---|---|---|
| | uncorrected | corrected | uncorrected | corrected |
| $\Omega_{\rm m0}$ | $0.288^{+0.107}_{-0.087}$ | $0.282^{+0.109}_{-0.086}$ | $0.286^{+0.111}_{-0.090}$ | $0.267^{+0.114}_{-0.088}$ |
| $w$ | $-1.159^{+0.610}_{-0.360}$ | $-1.132^{+0.571}_{-0.340}$ | $-1.112^{+0.565}_{-0.354}$ | $-1.074^{+0.504}_{-0.312}$ |
| $M$ | $-19.201^{+0.104}_{-0.078}$ | $-19.195^{+0.099}_{-0.076}$ | $-19.189^{+0.098}_{-0.076}$ | $-19.202^{+0.092}_{-0.071}$ |
| $\alpha$ | $1.254^{+0.121}_{-0.125}$ | $1.285^{+0.122}_{-0.124}$ | $1.243^{+0.121}_{-0.125}$ | $1.273^{+0.126}_{-0.127}$ |
| $\beta$ | $3.007^{+0.166}_{-0.170}$ | $2.987^{+0.166}_{-0.174}$ | $2.969^{+0.167}_{-0.172}$ | $3.087^{+0.172}_{-0.177}$ |

**Table 1:** Table quoted from Sakakibara et al. (2019). Best-fit values of each parameters estimated by MCMC method. We adopt the median values as the best fit values.

unchanged before and after the correction while for the DEmP, they are changed by $\sim 3\%$.

Jönsson et al. (2008) carry out a simulation to study the effect of lensing magnification and find that the lensing magnification biases in cosmological parameters by $\Delta\Omega_{\rm m0} = \Omega_{\rm m0}^{\rm lens} - \Omega_m \approx -0.005$ and $\Delta w = w^{\rm lens} - w \approx -0.005$ for 70 SNLS SNe. Our results read $\Delta\Omega_{\rm m0} = -0.001$ and $\Delta w = -0.001$ for Mizuki and $\Delta\Omega_{\rm m0} = -0.039$ and $\Delta w = 0.111$ for DEmP. The results for Mizuki are consistent with Jönsson et al. (2008), while they are inconsistent for DEmP. Also, Sarkar et al. (2008) generate mock SN samples to estimate the effect of gravitational lensing on $w$ and found that the bias on $w$ due to lensing magnification is less than 1%. They found that lensing convergences are not affect the central values and uncertainties on $\Omega_{\rm m0}$ and $w$.

## 5. Summary

In this paper we study the effect of gravitational magnification on the measurement of the cosmological parameters through type Ia SNe. To evaluate the magnification, we apply two different method: one from the convergence field measured by the shape distortion of the galaxies using HSC with superb image quality, the other from direct measurement of the mass using foreground galaxy distribution. Since the convergence measurement is too noisy to estimate the local magnification effect, we do not find any significant correlation between observed Hubble residual and magnification. However, with higher density sampling of galaxies in the future weak lensing surveys, such as LSST or EUCLID, the measurement will be improved. For the direct measurement of the magnification, we see very weak correlation between Hubble residual and the magnification. The largest uncertainty for this measurement arise from the photo-z uncertainty and stellar mass measurement. We compare two different photo-z codes Mizukia template fitting code and DEmPan empirical method and DEmPexhibits larger dispersion in the measurement of the magnification as the stellar mass measurement of DEmPis larger than that from Mizuki.

Finally, we correct the distance modulus for the magnification for individual SNe and find that the effect of magnification on the cosmological parameter estimation, $\Omega_m, w$ are at most 3% which is marginally consistent with previous works (Jönsson et al., 2008; Sarkar et al., 2008). The future

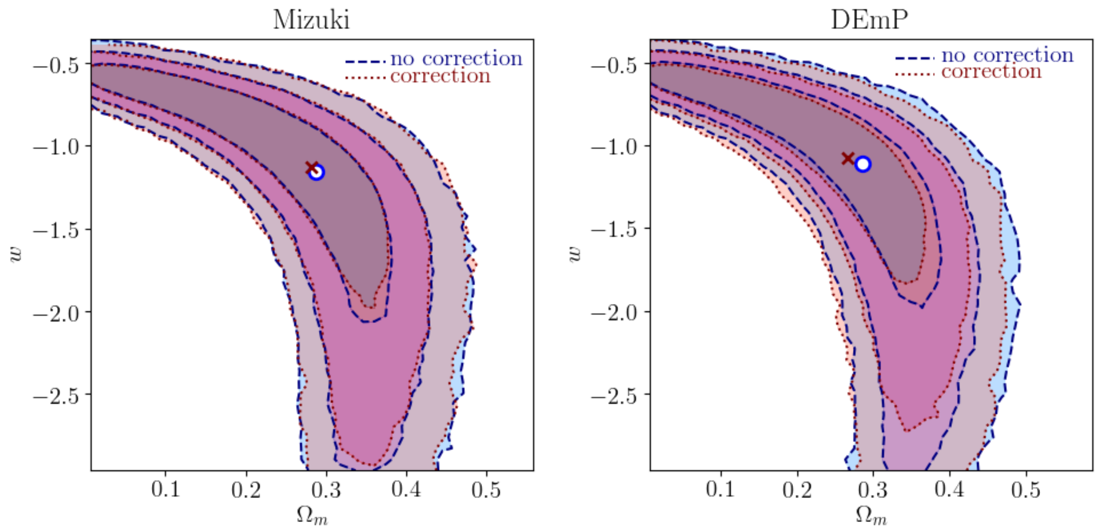


**Figure 2:** Figure quoted from Sakakibara et al. (2019). Constraints on $\Omega_{\rm m0}$ and $w$ from SNe sample corrected for magnification (red dotted) and not corrected (blue dashed). From inner to outer lines, they are 68.3%, 95.5% and 99.7% confidence regions of $\Omega_{\rm m0}$ and $w$, respectively. The blue circles and red crosses show the best-fit values for no correction and correction.

optical imaging surveys will detect higher redshift SNe which cause larger magnification and the impact of the magnification on the cosmological analysis will become more important.

## References

Astier P. et al., 2006, A&A, 447, 31

Behroozi P. S., Conroy C., Wechsler R. H., 2010, ApJ, 717, 379

Conley A. et al., 2011, ApJS, 192, 1

Conley A. et al., 2008, ApJ, 681, 482

Dawson K. S. et al., 2009, AJ, 138, 1271

Duffy A. R., Schaye J., Kay S. T., Dalla Vecchia C., 2008, MNRAS, 390, L64

Filippenko A. V., Li W. D., Treffers R. R., Modjaz M., 2001, in Astronomical Society of the Pacific Conference Series, Vol. 246, IAU Colloq. 183: Small Telescope Astronomy on Global Scales, Paczynski B., Chen W.-P., Lemme C., eds., p. 121

Frieman J. A., 1996, Comments on Astrophysics, 18, 323

Frieman J. A. et al., 2008, AJ, 135, 338

Garnavich P. M. et al., 1998, ApJL, 493, L53

Grogin N. A. et al., 2011, ApJS, 197, 35

Guy J. et al., 2007, A&A, 466, 11

Guy J. et al., 2010, A&A, 523, A7

Hsieh B. C., Yee H. K. C., 2014, ApJ, 792, 102

Jönsson J., Kronborg T., Mörtsell E., Sollerman J., 2008, A&A, 487, 467

Kaiser N., Squires G., 1993, ApJ, 404, 441

Kronborg T. et al., 2010, A&A, 514, A44

Mandelbaum R. et al., 2018, PASJ, 70, S25

Mandelbaum R. et al., 2008, MNRAS, 386, 781

Miyazaki S. et al., 2018, PASJ, 70, S1

Oguri M. et al., 2018, PASJ, 70, S26

Perlmutter S. et al., 1999, ApJ, 517, 565

Riess A. G. et al., 1998, AJ, 116, 1009

Sakakibara H., Nishizawa A. J., Oguri M., Tanaka M., Hsieh B.-C., Wong K. C., 2019, MNRAS, 486, 4365

Sarkar D., Amblard A., Holz D. E., Cooray A., 2008, ApJ, 678, 1

Takada M., Jain B., 2003a, MNRAS, 340, 580

Takada M., Jain B., 2003b, MNRAS, 344, 857

Takahashi R., Hamana T., Shirasaki M., Namikawa T., Nishimichi T., Osato K., Shiroyama K., 2017, ApJ, 850, 24

Tanaka M., 2015, ApJ, 801, 20

Tanaka M. et al., 2018, PASJ, 70, S9